Published in final edited form as:

ACS Chem Neurosci. 2019 August 21; 10(8): 3671–3681. doi:10.1021/acschemneuro.9b00248.

Cholesterol Biosynthesis and Uptake in Developing Neurons

Thiago C. Genaro-Mattos[†], **Allison Anderson**[†], **Luke B. Allen**[‡], **Zeljka Korade**[*,‡], **Károly Mirnics**[*,†]

[†]Munroe-Meyer Institute for Genetics and Rehabilitation, University of Nebraska Medical Center, Omaha, Nebraska 68105, United States

[‡]Department of Pediatrics, College of Medicine, University of Nebraska Medical Center, Omaha, Nebraska 68198, United States

Abstract

Brain cholesterol biosynthesis, a separate and distinct process from whole-body cholesterol homeostasis, starts during embryonic development. To gain a better understanding of the neuronal and glial contributions to the brain cholesterol pool, we studied this process in control, *Dhcr7*$^{-/-}$, and *Dhcr24*$^{-/-}$ cell cultures. Our LC-MS/MS method allowed us to measure several different sterol intermediates and cholesterol during neuronal differentiation. We found that developing cortical neurons rely on endogenous cholesterol synthesis and utilize ApoE-complexed cholesterol and sterol precursors from their surroundings. Both developing neurons and astrocytes release cholesterol into their local environment. Our studies also uncovered that developing neurons produced significantly higher amounts of cholesterol per cell than the astrocytes. Finally, we established that both neurons and astroglia preferentially use the Bloch sterol biosynthesis pathway, where desmosterol is the immediate precursor to cholesterol. Overall, our studies suggest that endogenous sterol synthesis in developing neurons is a critical and complexly regulated homeostatic process during brain development.

Graphical Abstract

[*]**Corresponding Authors:** karoly.mirnics@unmc.edu. zeljka.korade@unmc.edu.

Author Contributions

Study design: K.M., T.G-M., and Z.K.; funding: K.M.; LC-MS/MS analysis: T.G.-M.; GC-MS analysis: T.G.-M.; immunocytochemistry, imaging, and cell count: Z.K., T.G.-M. and L.B.A.; mouse colony maintenance and mouse dissection: A.A., L.B.A., and Z.K.; cell culture preparation, sterol extraction: Z.K., T.G.-M., A.A.; statistical analysis: T.G.-M.; writing of manuscript: T.G.-M., Z.K., and K.M.; final version read and approved by all authors.

Supporting Information

The Supporting Information is available free of charge on the ACS Publications website at DOI: 10.1021/acschemneuro.9b00248.

Experimental design and raw data on cell count associated with Figure 1 E,F (PDF)

The authors declare no competing financial interest.

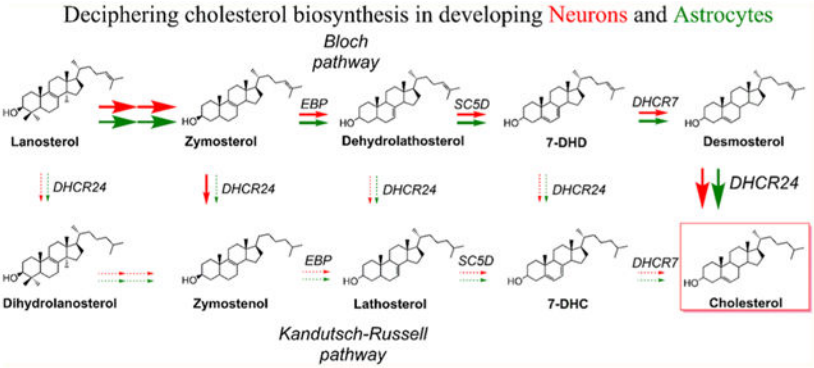

Keywords

Sterol biosynthesis; cholesterol; desmosterol; developing neurons; astrocytes; LC-MS/MS; Dhcr7; Dhcr24

INTRODUCTION

Although the human brain accounts only for about 2% of total body weight, it contains as much as 25% of the body's cholesterol and cholesterol derivatives.[1,2] The metabolism of brain cholesterol differs markedly from that of other tissues, and it fully relies on *de novo* synthesis, as the blood-brain barrier prevents the uptake of cholesterol from the circulation.[1,3] Sterol homeostasis disturbances are critical components of many brain disorders.[4] Dysfunction of the cholesterol biosynthesis pathways and/or metabolism leads or contributes to a number of neurodevelopmental and neuro-degenerative disorders such as Smith-Lemli-Opitz Syndrome (SLOS),[4–6] Niemann-Pick type C (NPC) disease,[7] desmosterolosis,[8,9] Huntington's disease,[10] and Alzheimer's disease.[11] Intact cholesterol metabolism is also essential for normal function of the adult brain: in the elderly, high cholesterol is associated with better memory function, while low cholesterol is associated with an increased risk for depression.[12–16] The function of cholesterol in the CNS extends beyond being a structural component of cellular membranes and lipid rafts: it is required for synapse and dendrite formation, axonal guidance, and serves as a precursor for various biosynthetic pathways.[17–22]

Cholesterol biosynthesis occurs by the same mechanism across all tissues, in two parallel and interlinked processes involving a series of enzymatic reactions, named Kandutsch-Russell (KR) and Bloch pathways.[23,24] In the brain, it has been proposed that neurons preferentially use the KR pathway, while glia are reliant on the Bloch pathway, but there has been a limited amount of experimental evidence to support this claim.[25]

Neurons express genes encoding cholesterol biosynthesis enzymes,[26] but it is widely believed that the main sterol synthesis in the adult brain is performed by glial cells.[17,27] In contrast, it appears that developing neurons heavily rely on their endogenous cholesterol biosynthesis and that this process is critical for their normal function and survival.[4,28] In support of this, in *Dhcr7*$^{-/-}$ and *Dhcr24*$^{-/-}$ mice, developing neurons accumulate cholesterol

precursors, with very little or no cholesterol present. However, since the mice do not live past the first day, the long-term consequence of lack of neuronal cholesterol is not known.

In our previous studies, we have used an improved, rapid, and sensitive LC-MS/MS method for quantitation of cholesterol biosynthetic precursors in cell culture, tissues, and plasma.[29] This technological advance allowed us to comprehensively test endogenous sterol synthesis in developing brain cells and assess the secretion process. Our study was set up to answer six questions related to cholesterol biosynthesis in developing neurons: (1) Do developing neurons have an active *de novo* cholesterol synthesis? (2) If so, how extensive is cholesterol biosynthesis in developing neurons, and how does it compare to astroglial sterol biosynthesis? (3) How steady is neuronal and astroglial sterol biosynthesis over development? (4) Do neurons and glia secrete cholesterol into their surrounding? (5) Do developing neurons and astroglia take up cholesterol from exogenous sources? (6) Do developing neurons and astroglia preferentially use the Kandutsch-Russell or Bloch pathway for their sterol biosynthesis?

RESULTS AND DISCUSSION

Neuronal and Astrocytic Cultures.

To determine the contribution of neuronal and glial cells to sterol synthesis in the developing brain, we prepared neuronal and astrocytic cultures from E18 cortex. A detailed experimental design is presented in the Supporting Figure 1, with representative images of neuronal and astrocytic cultures in panels C and D, respectively, of Figure 1. In order to normalize sterol measurements and control for cell viability, neurons and astrocytes were counted on an ImageXpress Pico. Total cell number was assessed at the beginning of the experiment and at different experimental time points. Astrocytic cell count increased from 3 days in culture (DIC3) to DIC9, suggesting that these cells were dividing (Figure 1B). Since neurons differentiated but did not divide, neuronal cultures presented similar cell count values at all-time points (Figure 1A). Rather, neurons developed elaborate arborization over time, as seen by immunocytochemistry (Figure 1C).

Immunocytochemistry was used to determine if neuronal cultures contained astrocytes and if astrocytic cultures contained neurons using MAP2 and GFAP antibodies at DIC6 (Supplemental Table 1). The imaging of the neuronal cultures revealed that 2.4% of the cells corresponded to astrocytes (Figure 1E). A similar assessment of the purity of astrocytic cultures revealed that 88.9% of the cells were astrocytes (Figure 1F).

Developing Cortical Neurons Synthesize Cholesterol.

In order to investigate their endogenous cholesterol synthesis, neurons and astrocytes were cultured in cholesterol-free medium for 3, 6, and 9 days. The sterol profile (cholesterol, 7-DHC, desmosterol, and lanosterol) for both cell types was assessed by LC-MS/MS (Figure 2). Lanosterol is the first intermediate that contains the four-ring structure present in cholesterol in the biosynthesis pathway, while desmosterol and 7-DHC are immediate precursors to cholesterol. We found that cholesterol is the most abundant sterol in the neurons followed by desmosterol, while 7-DHC was present at very low levels. Comparison

between sterol synthesis in neurons and astrocytes revealed significant differences between the two cell types. Namely, cholesterol accumulation was observed in a time-dependent manner in cortical neurons, indicating an active sterol biosynthesis (Figure 2A). In contrast, cholesterol levels in primary astrocytes decreased slightly over the course of 9 days (Figure 2B).

In primary neurons, all analyzed intermediates also increased in a time-dependent manner (Figure 2C,E,G), further confirming an active endogenous sterol biosynthesis. Astrocytes, on the other hand, presented a quite different pattern, with no detectable changes in 7-DHC (Figure 2D) and a decrease in both desmosterol and lanosterol levels from DIC3 to DIC9 (Figure 2F,H). These results indicate cell-specific cholesterol metabolism (or homeostasis), which are likely to be driven by their distinct developmental trajectory.

Accumulation of Sterol Intermediates in Dhcr7$^{-/-}$ and *Dhcr24*$^{-/-}$ Neurons.

The use of primary neuronal cultures with defective cholesterol synthesis enzymes allows us to assess the consequences of their absence on cholesterol biosynthesis. In *Dhcr7*$^{-/-}$ cells, 7-DHC is highly elevated, a biochemical condition resulting in Smith-Lemli-Opitz Syndrome (SLOS).[4,30,31] In *Dhcr24*-deficient cells, on the other hand, desmosterol is highly elevated, a biochemical feature linked with the disorder desmosterolosis.[9,32,33] We compared the cholesterol, desmosterol and 7-DHC steady-state levels in control, *Dhcr7*$^{-/-}$ (*Dhcr7*$^{T93M/T93M}$) and *Dhcr24*-deficient neurons at DIC3 (Figure 3). The profile of these three sterols is dramatically different in the neuronal cultures. As expected, control neurons have more cholesterol than both mutant cells (Figure 3A). In contrast, desmosterol is present at the highest levels in *Dhcr24*-deficient cells (Figure 3B), whereas 7-DHC is the highest in *Dhcr7*$^{-/-}$ neurons (Figure 3C). Importantly, in *Dhcr24*-deficient neurons, cholesterol is completely replaced by desmosterol. These results further suggest that neurons can independently synthesize cholesterol and that their sterol profiles reflect different mutations in the biosynthetic pathway.

Desmosterol Replaces Cholesterol in a Time-Dependent Manner in Dhcr24$^{-/-}$ Neurons.

We also performed a time -course analysis of the cholesterol and desmosterol levels in *Dhcr24*$^{+/+}$, *Dhcr24*$^{\pm}$, and *Dhcr24*$^{-/-}$ neurons (Figure 4). The steady-state levels of cholesterol and desmosterol in *Dhcr24*$^{+/+}$ increased from DIC3 to DIC6. In *Dhcr24*$^{-/-}$ neurons, on the other hand, cholesterol levels remained unchanged from DIC3 to DIC6 (Figure 4A), with a great increase in desmosterol (Figure 4B). As observed in Figure 3, desmosterol completely replaces cholesterol in *Dhcr24*$^{-/-}$ neurons at both time points investigated in our study. Sterol levels in *Dhcr24*$^{\pm}$ neurons were intermediate between levels seen in control and *Dhcr24*$^{-/-}$ neurons. These results also suggest that the steady-state levels observed in mutant cells are concordant with sterol biochemical data in the corresponding genetic disorders.

Active *De Novo* Cholesterol Synthesis in Neurons.

The *de novo* cholesterol biosynthesis uses acetyl-CoA as building blocks to synthesize sterols.[3] Acetyl-CoA is generated upon glucose oxidation via the glycolysis pathway. To address the de novo synthesis in neuronal cells, we replaced glucose in the medium with

$^{13}C_6$-glucose and incubated *Dhcr24*$^{+/+}$, *Dhcr24*$^{\pm}$, and *Dhcr24*$^{-/-}$ neurons for 6 days. At DIC6, cells were analyzed for their ^{13}C-labeled sterol content (Figure 5). *Dhcr24*$^{+/+}$ neurons synthesized ^{13}C-cholesterol from $^{13}C_6$-glucose, while *Dhcr24*$^{-/-}$ neurons synthesized ^{13}C-desmosterol (Figure 5A,5B). Furthermore, *Dhcr24*$^{\pm}$ heterozygous neurons have intermediate levels of all sterols measured. Note that ^{13}C-7-DHC and ^{13}C-lanosterol are also observed in all neurons analyzed (panels C and D, respectively, of Figure 5). By monitoring the steady-state levels of ^{13}C-labeled sterols we can conclude that developing neurons have an active de novo cholesterol synthesis, which is further demonstrated by the accumulation of ^{13}C-desmosterol by *Dhcr24*$^{-/-}$ neurons.

Notably, sterol levels in our study (including cholesterol) are normalized for cell count, which allowed us to estimate cholesterol accumulation per cell in neurons and astrocytes. Our results show that there is a remarkable increase in de novo cholesterol synthesis (Figures 2, 4 and 5) and accumulation in neurons over time (Figure 6). We emphasize that these findings should be interpreted in the context of neuronal development. We know that neurons need cholesterol to differentiate, and cholesterol accumulation in neurons is essential for neurite arborization, which requires membrane synthesis and, therefore, more cholesterol. Thus, we propose that they can regulate their own sterol synthesis, rather than being fully dependent on exogenous sources in the developmental milieu.

Astrocytes Release More Cholesterol into the Medium than Neurons.

In neurons, cholesterol is essential for both differentiation and establishment of elaborate arborization. However, it is unknown if neurons produce excessive amounts of endogenous cholesterol, and if so, what happens with the excess of cholesterol in the cells? Since neurons and astrocytes were maintained in cholesterol-free medium, we were able to assess their release of cholesterol into the extracellular space (Figure 6). Cell culture media from both neurons and astrocytes were collected and analyzed for cholesterol content by LC-MS/MS between DIC3 and DIC6 (Figure 6B). We found that neurons released an average of 3.2 ± 0.3 nmol cholesterol/million cells, and astrocytes released 5.2 ± 0.6 nmol cholesterol/million cells ($p = 0.0378$). In addition, we observed that cholesterol accumulated in both cell types between DIC3 and DIC6 but not at the same magnitude: over 3 days, neurons accumulated 15-fold more cholesterol than astrocytes (Figure 6C). Interestingly, between DIC3 and DIC6 neurons released about 5% of the total cholesterol accumulated in the cell, while astrocytes released 1.6 times more cholesterol than their intracellular accumulation. These data suggest that neurons accumulate most of their newly synthesized cholesterol, whereas astrocytes secrete most of it, keeping only the cholesterol necessary for their normal functioning. Thus, it appears that astrocytes and neurons both significantly contributed to the pool of extracellular cholesterol, with astrocytes contributing more to it. It is noteworthy that total cholesterol synthesis by neurons and astrocytes is a sum of retained and released cholesterol. However, the balance between the endogenous retention and release to the extracellular surroundings during brain development is likely be dynamic, and is expected to largely depend on the composition of the extracellular milieu. In this context, it is also important to note that uncontrolled secretion and accumulation of cholesterol in the extracellular space could have detrimental effects on brain development. Therefore, it is

likely that cholesterol synthesis and secretion are tightly regulated and connected feedback processes, in a yet unknown fashion.

The overall results suggest that neurons and astrocytes have a distinct developmental cholesterol homeostasis: astrocytes did not accumulate cholesterol, which is perhaps a reflection of their biology in the studied conditions: since astrocytes divide in culture, the expansion of their cell membrane (adjusted to cell count) is limited.

Neuronal and Astrocytic Uptake of Exogenous Sterols.

In addition to synthesis and release, uptake of exogenous cholesterol by brain cells is another important step in maintaining CNS sterol homeostasis. To assess exogenous cholesterol uptake, free isotopically labeled cholesterol (D_7-Chol), D_7-Chol precomplexed with ApoE, and D_7-Chol precomplexed with BSA were added to the defined cholesterol-free cell culture medium, as illustrated in Figure 7A. No cell death and no morphological changes were observed with these supplementations. After 3 days of incubation, cells were counted, and LC-MS/MS analyses were conducted to assess the incorporation of D_7-chol by neurons and astrocytes (Figure 7). Only a small incorporation of free D_7-chol was observed in primary neuronal cultures, which we attribute to the ~3% of glial composition of the cultures. This suggests a negligible uptake of free exogenous cholesterol by developing cortical neurons. A clear difference was observed in astrocytes, where cholesterol uptake was prominent. Indeed, the incorporation of free D_7-chol by astrocytes was 30–40 times higher than the incorporation by neurons. Next, we performed a similar experiment with D_7-chol precomplexed with either ApoE or BSA. Both neurons and astrocytes were incubated for 3 days with D_7-chol alone, D_7-chol-ApoE and D_7-Chol-BSA, and the D_7-chol uptake was assessed by LC-MS/MS (Figure 7B,C). Precomplexing D_7-chol with ApoE led to a 30-fold increase in the D_7-chol uptake by neurons (Figure 7B). The same complexation with BSA increased by 5-fold the neuronal uptake, which suggest that neuronal uptake relies on the specific complexation with ApoE. The astrocytic uptake, on the other hand, was not affected by the D_7-chol complexation with either ApoE or BSA (Figure 7C). These results suggest that while astrocytic cholesterol uptake is independent of protein complexes, neuronal cholesterol uptake relies specifically on cholesterol-ApoE complexes.

Next, we tested the ability of neuronal and glial cells to utilize other sterol intermediates from the extracellular milieu and metabolize them into cholesterol. To address this, free isotopically labeled lanosterol ($^{13}C_3$−Lan), $^{13}C_3$−Lan precomplexed with ApoE and $^{13}C_3$−Lan precomplexed with BSA were added to the defined cholesterol-free medium, followed by the assessment of isotopically labeled cholesterol ($^{13}C_3$−Chol) (Figure 7D). This method has been previously used in neuronal cell lines and primary human fibroblasts to evaluate sterol synthesis.[34] No cell death and no morphological changes were observed with these $13C_3$−Lan supplementations. We observed that astrocytes take up free $^{13}C_3$−Lan and converted it into $^{13}C_3$−Chol (Figure 7F). Neuronal cultures, on the other hand, synthesized a negligible amount of $^{13}C_3$−Chol, further suggesting that neurons do not readily take up free cholesterol precursors (Figure 7E). As observed with the free D_7-cholesterol uptake, the incorporation of free lanosterol by astrocytes was 25–30 times higher than in neurons. A similar experiment was performed with $^{13}C_3$−Lan precomplexed with

either ApoE or BSA. Both neurons and astrocytes were incubated for 3 days with $^{13}C_3$−Lan alone, $^{13}C_3$−Lan-ApoE3, and $^{13}C_3$−Lan-BSA, and the $^{13}C_3$−Chol synthesis was assessed by LC-MS/MS (Figure 7E,F). Precomplexing $^{13}C_3$−Lan with either of the proteins did not facilitate its uptake and further conversion to $^{13}C_3$−Chol astrocytes (Figure 7F). On the hand, neuronal 13C_3−Lan uptake and conversion to $^{13}C_3$−Chol increased 40-fold with $^{13}C_3$−Lan complexed with ApoE (Figure 7E). It is worth mentioning that small levels of $^{13}C_3$-desmosterol were detected in astrocytic cultures, which further suggests that these cells are taking $^{13}C_3$−Lan and metabolizing it (data not shown). Altogether these results suggest that while neuronal sterol uptake is ApoE-complex-dependent, astrocytes can take up free sterols from extracellular milieu.

Beyond relying on their endogenous sterol synthesis, it is also noteworthy that developing neurons can take up ApoE-sterol complexes from the surrounding cells. The *de novo* synthesis and ApoE complexed cholesterol uptake might present two redundant and complementary mechanisms that jointly ensure essential neuronal access to cholesterol under the changing conditions of development or disease. The internal balance and regulation of these two processes is unknown at the current time, but it appears that both mechanisms are essential: previously published transgenic studies suggest that endogenous cholesterol synthesis by developing neurons is critical for brain development.[19] Yet, the relative contribution of these two mechanisms to cholesterol biosynthesis in neurons is likely to be dynamic, dependent on the developmental stage and the physiological/pathophysiological processes that they encounter. Furthermore, the sterol exchange between neurons and astrocytes is limited during embryonic development, since astrogenesis starts postnatally.[35,36] Therefore, despite the ability of embryonic neurons to take up ApoE-bound sterols, the occurrence of astrocytic support during embryonic development is unlikely.

Neurons and Astrocytes Synthesize Cholesterol through the Bloch Pathway.

As mentioned above, the conversion of lanosterol into cholesterol can occur through two parallel routes of biosynthesis, the Bloch and Kandutsch-Russell pathways.[37] Intermediates from these pathways differ from each other by the presence of a double bond at the C24 position. This double bond is reduced by the enzyme DHCR24, a step that could theoretically happen at any stage in the postlanosterol pathway. In order to investigate the existence of a preferential sterol biosynthesis pathway, we determined the sterol profile in cultured neurons and astrocytes at DIC6 (Figure 8A). Assessing postlanosterol intermediates (Bloch pathway: zymosterol, dehydrolathosterol, 7-DHD, and desmosterol; and KR pathway: dihydrolanosterol, zymostenol, lathosterol, and 7-DHC) by GC-MS allowed us to gain insight in the dynamics of cell-type specific cholesterol biosynthesis. This analysis revealed that neurons have higher levels of most intermediates, apart from 7-DHD and desmosterol that are found at higher levels in astrocytes. In addition, 93% and 98% of the sterol intermediates found in neurons and astrocytes, respectively, were part of the Bloch pathway (Figure 8C). More specifically, the most abundant sterols in neurons (in order of abundance) are cholesterol ≫ desmosterol ≫7-DHD = zymosterol = zymostenol > all other sterols. In astrocytes, a similar profile is observed where the most abundant sterols are cholesterol ≫ desmosterol ≫7-DHD > all other sterols. These profiles suggest that lanosterol is mostly converted into desmosterol and then to cholesterol via the Bloch

pathway, with minimal DHCR24 activity affecting earlier intermediates (Figure 8B). We can conclude that both neurons and astrocytes preferentially use the Bloch pathway to synthesize cholesterol, suggesting a very limited role of the KR biosynthesis pathway during brain development. This is a considerable departure of the currently held view, which states that glial cells primarily rely on the Bloch pathway, while neurons primarily utilize the KR pathway for their sterol biosynthesis.[25]

Although sterol biosynthesis could theoretically be synthesized by the two above-mentioned biosynthetic pathways, our findings suggest that the two pathways are not equally utilized in the developing brain cells. In all cell lines we have used so far (e.g., fibroblasts, Neuro2a cells, neurons, astrocytes),[34,38−40] cholesterol is the most abundant sterol followed by desmosterol, which indicates that all the investigated cell types in the brain and other tissues preferentially use the Bloch pathway, where desmosterol is the immediate precursor to cholesterol. While the DHCR24 enzyme can theoretically reduce the C24 double bond at any stage, our findings suggest that over 90% of its activity involves the conversion of desmosterol into cholesterol. The finding of preferential use of the Bloch pathway by developing neurons is also strongly supported by our assessment of the *de novo* synthesis with $^{13}C_6$-glucose, as the levels of ^{13}C-desmosterol (last intermediate in the Bloch pathway) are ~60 times higher than ^{13}C-7-DHC (last intermediate in the KR pathway) in WT-*Dhcr24*$^{+/+}$ neurons (Figure 5). However, literature data suggests that the balance of these two pathways might be dynamic[37] and may change under pathophysiological conditions: for instance, detection of novel sterol intermediates in a cancer cell line led to the initial discovery of the Kandutsch-Russell pathway.[24] To date, such data are not available for CNS disorders, and this should be a further topic of investigation.

CONCLUSIONS

Our results can be summarized as follows: (1) Developing neurons have an active *de novo* cholesterol synthesis. (2) Both developing neurons and astrocytes release cholesterol into their local environment. (3) Steady-state levels of cholesterol are higher in neurons than in astrocytes, with a significantly higher amount of cholesterol produced in neurons. (4) Neuronal endogenous sterol pool increases over time, while astrocytes maintain a strict control of their endogenous cholesterol homeostasis. (5) While exogenous sterol uptake in neurons is ApoE-complex-dependent, astrocytes can take up free sterols from the extracellular milieu. (6) Both neurons and astroglia preferentially use the Bloch pathway, where desmosterol is the immediate precursor to cholesterol.

Our studies also raise additional questions of interest, which will have to be tested in future studies. First, do other glial cells types (oligodendrocytes and microglia) also make their own cholesterol during development and contribute to the overall brain cholesterol homeostasis? Second, do different neuronal cell types have vastly different sterol synthesis[41] and/or cholesterol utilization from the extracellular space? This is likely to be true, as different brain regions have distinct sterol levels and express different levels of transcripts encoding sterol biosynthesis enzymes.[42,43] Third, our studies focused on developing neurons and did not address how sterol biosynthesis is regulated in the adult or aging brain. Clearly, cholesterol production, trafficking, and homeostasis is very different in the mature brain,

where adult neurons primarily rely on cholesterol produced by astrocytes.[44] Fourth, since mutations in sterol biosynthesis enzymes lead to devastating developmental disorders, do these mutations equally affect neurons and glia, or are the neuronal cells preferentially impacted by the disease process, as neurons mostly rely on their own sterol biosynthesis?

Finally, we believe that neuronal sterol biosynthesis during development is a critical, yet poorly understood and still underappreciated area of neuroscience research. Deciphering the time course of developmental brain cholesterol synthesis and regulation might significantly advance our understanding of diseases in which disturbed cholesterol biosynthesis, clearance, and turnover are an integral part of the pathological processes.

METHODS

Chemicals.

Unless otherwise noted, all chemicals were purchased from Sigma-Aldrich Co (St. Louis, MO). HPLC-grade solvents were purchased from VWR BDH chemicals (Radnor, PA). All sterol standards, natural and isotopically labeled, used in this study are available from Kerafast, Inc. (Boston, MA). Ergosterol was purchased from TCI America (Portland, OR). $^{13}C_6$-glucose was purchased from Cambridge Isotope Laboratories, Inc. ApoE3 (no. 350–02) was purchased from PeproTech, Rocky Hill, NJ.

Mouse Experiments.

Adult mice, stock 00664 C57Bl/6J and B6.129S5-*Dhcr24*^{tm1lex}/*SbpaJ*, stock 012564 were purchased from the Jackson Laboratory (Bar Harbor, ME). T93M mice were obtained from FD Porter.[30] These mice have a mutation in both *Dhcr7* alleles at c.278C > T, a mutation equivalent to the human T93M missense mutation. The T93M mutation is the most common missense mutation described in patients with Smith-Lemli-Opitz Syndrome (SLOS).[30,45] These mice have a limited residual cholesterol synthesis, and they survive into adulthood and breed. The brain tissue of T93M embryos has highly elevated 7-DHC levels.[30] For simplicity, throughout the results we refer to these mice as Dhcr7$^{-/-}$. *Dhcr24*-KO mice have a 249 bp deletion in exon 1 and the brain has high levels of desmosterol.[9] The colony is maintained by breeding WT and *Dhcr24*-heterozygous (Het) mice. Breeding *Dhcr24*-Het with *Dhcr24*-Het mice gives ~25% *Dhcr24*-KO mice that die shortly after birth.

All mice were housed under a 12 h light-dark cycle at constant temperature (25 °C) and humidity with ad libitum access to food (Teklad LM-485 Mouse/Rat Irradiated Diet 7912) and water in Comparative Medicine at UNMC, Omaha, NE. Embryonic and newborn mice were used for the study. All procedures were performed in accordance with the Guide for the Humane Use and Care of Laboratory Animals. The use of mice in this study was approved by the Institutional Animal Care and Use Committee of UNMC.

Primary Neuronal Cultures.

Primary cortical neuronal cultures for wild-type and *Dhcr7*$^{-/-}$ experiments were prepared from E18 mice as previously described.[26,46] Neuronal cultures used for *Dhcr24*$^{-/-}$ experiments were prepared from E15 brains. Briefly, the brain was placed in prechilled

HBSS solution (without Ca^{2+} or Mg^{2+}), and two cortexes were dissected and cut with scissors into small chunks of similar sizes and transferred to Trypsin/EDTA (0.5%) for 25 min at 37 °C. Trypsin was inactivated by adding Trypsin Inhibitor (Sigma T6522) for 5 min. Samples were then spun at 100*g*. The tissue was resuspended in Neurobasal medium with B-27 supplement (Gibco no. 17504–044) and then triturated with a fire-polished Pasteur pipet. The cells were pelleted by centrifugation for 5 min at 80*g*. The cell pellet was resuspended in Neurobasal medium with B-27 supplement, and the cells were counted. The cells were plated on poly-D-lysine coated 96-well plates at 60 000 cells/well. The growth medium was Neurobasal medium with B-27 supplement, Glutamax and 3 μM cytosine arabinoside. Cells were incubated at 37 °C, 5% CO_2 for 3, 6, or 9 days. At the end point of the incubation, 10 μL of Hoechst dye was added to all wells in the 96-well plate, and the total number of cells was counted using an ImageXpress Pico. After removing the medium, wells were rinsed twice with 1× PBS and then stored at −80 °C for lipid analysis. All samples were analyzed within 2 weeks of freezing.

Primary Astrocytic Cultures.

After plating the required number of cells for neuronal cultures, leftover cells were plated in 100 mm dishes at a density 10×10^6 per tissue culture plate in DMEM with 10% FBS. Under these conditions, astrocytes adhere and divide and completely populate the plate within 10–14 days. Once the plates were full, they were rinsed using the cold jet method.[47] The astrocytes were trypsinized and plated in 96-well plates in DMEM plus 10% FBS at 30 000 cells/well. The following day the medium was completely changed, and astrocytes were grown in Neurobasal medium with B-27 supplement (Gibco no. 17504–044) in the absence of cholesterol (same medium as neuronal cells without cytosine arabinoside). Cells were incubated at 37 °C, 5% CO_2 for 3, 6, or 9 days. At the end point of the incubation, 10 μL of Hoechst dye was added to all wells in the 96-well plate, and the total number of cells was counted using an ImageXpress Pico. After removing the medium, wells were rinsed twice with 1× PBS and then stored at −80 °C for lipid analysis. All samples were analyzed within 2 weeks of freezing.

De Novo Cholesterol Synthesis Assessed by $^{13}C_6$-Glucose Experiments.

Neuronal cells were cultured in Neurobasal medium (without glucose − Gibco no. A24775–01), B27-supplement, and 10 mM of $^{13}C_6$-glucose. The replacement of natural glucose by $^{13}C_6$-glucose in the medium provided labeled carbons to be used in the biosynthesis of fresh sterols, as described previously.[38] To monitor freshly synthesized ^{13}C-labeled sterols, we selected one isotope for each sterol (e.g. $^{13}C_4$-7-DHC, SRM transition 564 → 369) to be used in the analyses and calculated a response factor to account for the sum of every possible isotope and, hence, the total amount of isotopically labeled sterol formed. This correction factor was used for every sterol analysis reported in this study ($^{13}C_4$-cholesterol, SRM transition 373 → 373, $^{13}C_4$-desmosterol, SRM transition 596 →564).

Immunocytochemistry and Imaging.

At the end of incubation, the cultures were processed for immunocytochemistry. Briefly, wells were rinsed with 1× PBS and fixed with 4% *p*-formaldehyde. After removing p-formaldehyde, wells were rinsed again with 1× PBS and blocked for 30 min at room

temperature in the blocking buffer (10% FBS in 1× PBS plus 0.1% saponin). Primary antibodies were then added (MAP2 - Cell Signaling no. D5G1; GFAP - ABCAM no. ab4674) and incubated overnight at 4 °C. Primary antibodies were removed, and wells were rinsed with 1× PBS. Secondary antibodies were added, and samples were incubated for 30 min at room temperature. The following secondary antibodies were used: Jackson ImmunoResearch Cy3-conjugated AffiniPure Donkey antirabbit; and AlexaFluor 488-conjugated AffiniPure Donkey antichicken. Since the experiments were conducted in a 96-well plate format, the following conditions were prepared: (a) MAP2 only; (b) GFAP only; (c) MAP2 plus GFAP; in all three conditions, their respective secondary antibodies were used. Additional controls were used where wells were incubated with secondary antibodies only (no primary antibodies were present). After rinsing, plates were imaged on an ImageXpress Pico Automated Cell Imaging System using 4× and 10× Fluotar objectives in the Cy3, FITC, DAPI, and bright field channels. Images were acquired with CellReporterXpress software. Images acquired at 10× were stitched from multiple adjacent fields within each well.

To determine the astrocytic content in neuronal cultures, 4 wells were imaged at 4×, taking 4 images per well to cover the whole well, for a total of 16 images. Astrocytes were counted using the cell counting algorithm in CellReporterXpress, counting only cells that were FITC-positive (GFAP). Astrocytic and neuronal nuclei were counted using the same algorithm but set to count DAPI positive nuclei from the Hoechst stain. The astrocyte content is reported as the average number of astrocytes counted in the FITC channel over the average number of nuclei counted in the DAPI channel. Analogously, to determine the neuronal content in astrocytic cultures, 3 wells were imaged at 10× in both the DAPI and Cy3 channels, stitching the individual fields of view within one well. From each well, 9 individual fields of view were captured covering 53.7% of the total well area, resulting in 27 individual images total. These fields of view were confirmed to be representative of the whole well by manual review. Neurons were counted using the cell counting algorithm in CellReporterXpress with the parameters set to count only the brightest Cy3 positive (MAP2) cells that would indicate neurons. The accuracy of the algorithm's selection of neurons was manually reviewed to confirm its accuracy. The neuronal content is reported as the average number of neurons counted in the Cy3 channel over the average number of nuclei counted in the DAPI channel.

Sterol Complexation with Either ApoE or BSA.

To investigate the uptake of sterol-protein complexes by neurons and astrocytes, either D_7-cholesterol or $^{13}C_3$-lanosterol were complexed with ApoE or BSA as described previously.[48] Briefly, isotopically labeled sterols were mixed with the proteins in PBS solution and incubated overnight at 37 °C under agitation. Complexed sterols were then added to the medium, and the neuronal and astrocytic uptake was assessed by LC-MS/MS.

Lipid Extraction and Sample Preparation.

Sterol levels were analyzed in individual wells and, for most experiments, cellular levels correspond to 8–12 technical replicates. After rinsing plates with 1× PBS (or removing previously frozen plates from −80 °C freezer) 200 μL of MeOH containing the internal

standard was added, as reported previously.[34,38] The plate was placed on an orbital shaker for 30 min at room temperature and centrifuged for 10 min using a Sorvall swing rotor. An aliquot (100 μL) of the supernatant was transferred to a PTAD-predeposited plate, sealed with Easy Pierce Heat Sealing Foil followed by 30 min agitation at room temperature, and analyzed by LC-MS/MS (as described in a following section). For measurements of sterol release into the cell culture medium, media from 4 individual wells were combined, and the data shown in Figure 3B correspond to 3 technical replicates. After collecting the medium, samples were centrifuged at 10 000*g* for 10 min to clear the medium from any potential cellular debris. Additional control experiments revealed that the method we used was as efficient in removing cellular debris as pelleting. Sterols were extracted using the Folch method as described previously.[29] Values were normalized by average cell count and reported as nmol/million cells. For GC-MS analysis, single wells were extracted with 200 μL of MeOH containing an internal standard cocktail as previously described (D_7-cholesterol, D_7-7-DHC,[13] C_3-desmosterol, and $^{13}C_3$-lanosterol).[38] Samples were dried on a SpeedVac concentrator and stored at −80 °C for GC-MS analysis.

LC-MS/MS (SRM) Analyses.

Extracted sterols were derivatized with 4-phenyl-1,2,4-triazoline-3,5-dione (PTAD) as described previously[38] and placed in an Acquity UPLC system equipped with ANSI-compliant well plate holder coupled to a Thermo Scientific TSQ Quantis mass spectrometer equipped with an APCI source. Then 5 μL was injected onto the column (Acquity BEH C18 1.7 μm,2.1 mm × 50 mm) with 100% MeOH (0.1% v/v acetic acid) mobile phase for 1.0 min runtime at a flow rate of 500 μL/min. Natural sterols were analyzed by selective reaction monitoring (SRM) using the following transitions: Chol 369 → 369, 7-DHC 560 → 365, desmosterol 592 → 560, lanosterol 634 → 602, with retention times of 0.7, 0.4, 0.3, and 0.3 min, respectively. SRM for $^{13}C_3$-cholesterol ($^{13}C_3$−Chol) was set to 373 → 373, and the values were corrected for the natural isotopic distribution. SRM for D_7-cholesterol (D_7-Chol) was set to 376 → 376. To quantitate ^{13}C-labeled sterols synthesized from $^{13}C_6$-glucose, we monitored the following SRM transitions: $^{13}C_4$-cholesterol 373 → 373; $^{13}C_4$-7-DHC 564 → 369; $^{13}C_4$-desmosterol 596 → 564. For quantitation, 0.3 nmol of ergosterol was used as the internal standard, and the SRM was set to 572 → 377. Response factors for Chol, 7-DHC, Des, and Lan in relation to ergosterol were determined to allow for a proper quantitation. Final sterol numbers are reported as nmol/million cells.

GC-MS Analyses.

Dried lipid samples were derivatized with *N,O*-bis(trimethylsilyl)trifluoroacetamide (BSTFA), and 5 μL was injected onto the column (SPB-5, 0.25 μm, 0.32 mm × 30 m) with the following temperature program: 180 °C was held for 1 min; then increased to 250 °C at 20 °C/min; then raised to 300 °C at 4 °C/min and kept for 7 min.[49] Selected sterol intermediates were analyzed by extracted ion chromatogram (EIC) using the following values: lathosterol (*m/z* 458), zymostenol (*m/z* 458), dihydrolanosterol (*m/z* 395), dehydrolathosterol (*m/z* 456), zymosterol (*m/z* 456), 7-dehydrodesmosterol (7-DHD - *m/z* 349), and D_7-Chol (*m/z* 465). Final sterol numbers were calculated using D_7-Chol as the internal standard. Response factors were calculated for each sterol and used to calculate the total amount.

Statistical Analyses.

Statistical analyses were performed using Graphpad Prism 7 for Windows and Microsoft Excel. Unpaired two-tailed *t* tests were performed for individual comparisons between two groups. The Welch's correction was employed when the variances between the two groups was significantly different. Ordinary one-way ANOVA and multiple comparisons with Tukey corrections were performed for comparisons between three or more groups. The *p* values for statistically significant differences are highlighted in the figure legends.

Supplementary Material

Refer to Web version on PubMed Central for supplementary material.

ACKNOWLEDGMENTS

This work was supported by The National Institutes of Health NIMH R01 MH110636 (KM) and R01 MH067234 (KM). The authors would like to thank Dr. William Rizzo (UNMC, Omaha) for allowing the use of the GC-MS instrument and for a critical review of the manuscript. The authors would also like to thank Dr. Forbes Porter (NIH) for donating the T93M mice used in this study.

ABBREVIATIONS

Dhcr7	7-dehydrocholesterol reductase
Dhcr24	24-dehydrocholesterol reductase
ApoE	apolipoprotein E
SLOS	Smith-Lemli-Opitz Syndrome
NPC	Niemann-Pick type C disease
CNS	central nervous system
KR	Kandutsch-Russell
LC-MS/MS	liquid chromatography coupled with tandem mass spectrometry
7-DHC	7-dehydrocholesterol
Het	heterozygous
KO	knockout
HBSS	Hanks-balanced salt solution
DIC	days in culture
MAP2	microtubulin associated protein 2
GFAP	glial fibrillary acid protein
BSA	bovine serum albumin
MeOH	methanol

PBS	phosphate buffered saline
PTAD	4-phenyl-1:2,4-triazoline-3,5-dione
Chol	cholesterol
$^{13}C_3$−Chol	$^{13}C_3$-cholesterol
D_7-Chol	D_7-cholesterol
GC-MS	gas chromatography coupled with mass spectrometry
BSTFA	*N,O*-bis(trimethylsilyl)trifluoroacetamide
EIC	extracted ion chromatogram
7-DHD	7-dehydrodesmosterol
$^{13}C_3$-Lan	$^{13}C_3$-lanosterol

REFERENCES

(1). Dietschy JM, and Turley SD (2001) Cholesterol metabolism in the brain. Curr. Opin. Lipidol 12, 105–12. [PubMed: 11264981]

(2). Dietschy JM, and Turley SD (2004) Thematic review series: brain Lipids. Cholesterol metabolism in the central nervous system during early development and in the mature animal. J. Lipid Res 45, 1375–97. [PubMed: 15254070]

(3). Nes WD (2011) Biosynthesis of cholesterol and other sterols. Chem. Rev 111, 6423–51. [PubMed: 21902244]

(4). Porter FD, and Herman GE (2011) Malformation syndromes caused by disorders of cholesterol synthesis. J. Lipid Res 52, 6–34. [PubMed: 20929975]

(5). Porter FD (2000) RSH/Smith-Lemli-Opitz syndrome: a multiple congenital anomaly/mental retardation syndrome due to an inborn error of cholesterol biosynthesis. Mol. Genet. Metab 71, 163–74. [PubMed: 11001807]

(6). Smith DW, Lemli L, and Opitz JM (1964) A Newly Recognized Syndrome of Multiple Congenital Anomalies. J. Pediatr 64, 210–7. [PubMed: 14119520]

(7). Xie C, Turley SD, and Dietschy JM (1999) Cholesterol accumulation in tissues of the Niemann-pick type C mouse is determined by the rate of lipoprotein-cholesterol uptake through the coated-pit pathway in each organ. Proc. Natl. Acad. Sci. U. S. A 96, 11992–7. [PubMed: 10518564]

(8). Waterham HR, Koster J, Romeijn GJ, Hennekam RC, Vreken P, Andersson HC, FitzPatrick DR, Kelley RI, and Wanders RJ (2001) Mutations in the 3beta-hydroxysterol Delta24-reductase gene cause desmosterolosis, an autosomal recessive disorder of cholesterol biosynthesis. Am. J. Hum. Genet 69, 685–94. [PubMed: 11519011]

(9). Allen LB, Genaro-Mattos TC, Porter NA, Mirnics K, and Korade Z. 2019 Desmosterolosis and desmosterol homeostasis in the developing mouse brain. J. Inherit Metab Dis, in press.

(10). Valenza M, Leoni V, Tarditi A, Mariotti C, Bjorkhem I, Di Donato S, and Cattaneo E (2007) Progressive dysfunction of the cholesterol biosynthesis pathway in the R6/2 mouse model of Huntington's disease. Neurobiol. Dis 28, 133–42. [PubMed: 17702587]

(11). Wolozin B (2004) Cholesterol and the biology of Alzheimer's disease. Neuron 41, 7–10. [PubMed: 14715130]

(12). Knowles EEM, Curran JE, Meikle PJ, Huynh K, Mathias SR, Goring HHH, VandeBerg JL, Mahaney MC, Jalbrzikowski M, Mosior MK, Michael LF, Olvera RL, Duggirala R, Almasy L, Glahn DC, and Blangero J (2018) Disentangling the genetic overlap between cholesterol and suicide risk. Neuropsychopharmacology 43, 2556–2563. [PubMed: 30082891]

(13). Segoviano-Mendoza M, Cardenas-De La Cruz M, Salas-Pacheco J, Vazquez-Alaniz F, La Llave-Leon O, Castellanos-Juarez F, Mendez-Hernandez J, Barraza-Salas M, Miranda-Morales E, Arias-Carrion O, and Mendez-Hernandez E (2018) Hypocholesterolemia is an independent risk factor for depression disorder and suicide attempt in Northern Mexican population. BMC Psychiatry 18,7. [PubMed: 29334911]

(14). Cham S, Koslik HJ, and Golomb BA (2016) Mood, Personality, and Behavior Changes During Treatment with Statins: A Case Series. Drug Saf Case Rep 3, 1. [PubMed: 27747681]

(15). Raihan O, Brishti A, Molla MR, Li W, Zhang Q, Xu P, Khan MI, Zhang J, and Liu Q (2018) The Age-dependent Elevation of miR-335-3p Leads to Reduced Cholesterol and Impaired Memory in Brain. Neuroscience 390, 160–173. [PubMed: 30125687]

(16). Mast N, Lin JB, Anderson KW, Bjorkhem I, and Pikuleva IA (2017) Transcriptional and post-translational changes in the brain of mice deficient in cholesterol removal mediated by cytochrome P450 46A1 (CYP46A1). PLoS One 12, No. e0187168. [PubMed: 29073233]

(17). Barres BA, and Smith SJ (2001) Neurobiology. Cholesterol–making or breaking the synapse. Science 294, 1296–7. [PubMed: 11701918]

(18). Ferris HA, Perry RJ, Moreira GV, Shulman GI, Horton JD, and Kahn CR (2017) Loss of astrocyte cholesterol synthesis disrupts neuronal function and alters whole-body metabolism. Proc. Natl. Acad. Sci. U. S. A 114, 1189–1194. [PubMed: 28096339]

(19). Funfschilling U, Jockusch WJ, Sivakumar N, Mobius W, Corthals K, Li S, Quintes S, Kim Y, Schaap IA, Rhee JS, Nave KA, and Saher G (2012) Critical time window of neuronal cholesterol synthesis during neurite outgrowth. J. Neurosci 32, 7632–45. [PubMed: 22649242]

(20). Norlin M, and Wikvall K (2007) Enzymes in the conversion of cholesterol into bile acids. Curr. Mol. Med 7, 199–218. [PubMed: 17346171]

(21). Goritz C, Mauch DH, and Pfrieger FW (2005) Multiple mechanisms mediate cholesterol-induced synaptogenesis in a CNS neuron. Mol. Cell. Neurosci 29, 190–201. [PubMed: 15911344]

(22). Korade Z, and Kenworthy AK (2008) Lipid rafts, cholesterol, and the brain. Neuropharmacology 55, 1265–73. [PubMed: 18402986]

(23). Bloch K (1965) The biological synthesis of cholesterol. Science 150, 19–28. [PubMed: 5319508]

(24). Kandutsch AA, and Russell AE (1960) Preputial gland tumor sterols. 3. A metabolic pathway from lanosterol to cholesterol. J. Biol. Chem 235, 2256–2261. [PubMed: 14404284]

(25). Zhang J, and Liu Q (2015) Cholesterol metabolism and homeostasis in the brain. Protein Cell 6, 254–64. [PubMed: 25682154]

(26). Korade Z, Mi Z, Portugal C, and Schor NF (2007) Expression and p75 neurotrophin receptor dependence of cholesterol synthetic enzymes in adult mouse brain. Neurobiol. Aging 28, 1522–31. [PubMed: 16887237]

(27). Pfrieger FW (2003) Outsourcing in the brain: do neurons depend on cholesterol delivery by astrocytes? BioEssays 25, 72–8. [PubMed: 12508285]

(28). Michikawa M, and Yanagisawa K (1999) Inhibition of cholesterol production but not of nonsterol isoprenoid products induces neuronal cell death. J. Neurochem 72, 2278–85. [PubMed: 10349836]

(29). Liu W, Xu L, Lamberson C, Haas D, Korade Z, and Porter NA (2014) A highly sensitive method for analysis of 7-dehydrocholesterol for the study of Smith-Lemli-Opitz syndrome. J. Lipid Res 55, 329–37. [PubMed: 24259532]

(30). Correa-Cerro LS, Wassif CA, Kratz L, Miller GF, Munasinghe JP, Grinberg A, Fliesler SJ, and Porter FD (2006) Development and characterization of a hypomorphic Smith-Lemli-Opitz syndrome mouse model and efficacy of simvastatin therapy. Hum. Mol. Genet 15, 839–51. [PubMed: 16446309]

(31). Porter FD (2008) Smith-Lemli-Opitz syndrome: pathogenesis, diagnosis and management. Eur. J. Hum. Genet 16, 535–41. [PubMed: 18285838]

(32). FitzPatrick DR, Keeling JW, Evans MJ, Kan AE, Bell JE, Porteous ME, Mills K, Winter RM, and Clayton PT (1998) Clinical phenotype of desmosterolosis. Am. J. Med. Genet 75, 145–52. [PubMed: 9450875]

(33). Andersson HC, Kratz L, and Kelley R (2002) Desmosterolosis presenting with multiple congenital anomalies and profound developmental delay. Am. J. Med. Genet 113, 315–9. [PubMed: 12457401]

(34). Korade Z, Genaro-Mattos TC, Tallman KA, Liu W, Garbett KA, Koczok K, Balogh I, Mirnics K, and Porter NA (2017) Vulnerability of DHCR7(±) mutation carriers to aripiprazole and trazodone exposure. J. Lipid Res 58, 2139–2146. [PubMed: 28972118]

(35). Reemst K, Noctor SC, Lucassen PJ, and Hol EM (2016) The Indispensable Roles of Microglia and Astrocytes during Brain Development. Front. Hum. Neurosci 10, 566. [PubMed: 27877121]

(36). Vallejo M (2009) PACAP signaling to DREAM: a cAMP-dependent pathway that regulates cortical astrogliogenesis. Mol. Neurobiol 39, 90–100. [PubMed: 19238593]

(37). Mitsche MA, McDonald JG, Hobbs HH, and Cohen JC (2015) Flux analysis of cholesterol biosynthesis in vivo reveals multiple tissue and cell-type specific pathways. eLife 4, No. e07999. [PubMed: 26114596]

(38). Genaro-Mattos TC, Tallman KA, Allen LB, Anderson A, Mirnics K, Korade Z, and Porter NA (2018) Dichlorophenyl piperazines, including a recently-approved atypical antipsychotic, are potent inhibitors of DHCR7, the last enzyme in cholesterol biosynthesis. Toxicol. Appl. Pharmacol 349, 21–28. [PubMed: 29698737]

(39). Korade Z, Kim HY, Tallman KA, Liu W, Koczok K, Balogh I, Xu L, Mirnics K, and Porter NA (2016) The Effect of Small Molecules on Sterol Homeostasis: Measuring 7-Dehydrocholesterol in Dhcr7-Deficient Neuro2a Cells and Human Fibroblasts. J. Med. Chem 59, 1102–15. [PubMed: 26789657]

(40). Kim HY, Korade Z, Tallman KA, Liu W, Weaver CD, Mirnics K, and Porter NA (2016) Inhibitors of 7-Dehydrocholesterol Reductase: Screening of a Collection of Pharmacologically Active Compounds in Neuro2a Cells. Chem. Res. Toxicol 29, 892− 900. [PubMed: 27097157]

(41). Ko M, Zou K, Minagawa H, Yu W, Gong JS, Yanagisawa K, and Michikawa M (2005) Cholesterol-mediated neurite outgrowth is differently regulated between cortical and hippocampal neurons. J. Biol. Chem 280, 42759–65. [PubMed: 16267051]

(42). Zhang Y, Appelkvist EL, Kristensson K, and Dallner G (1996) The lipid compositions of different regions of rat brain during development and aging. Neurobiol. Aging 17, 869–75. [PubMed: 9363798]

(43). Soderberg M, Edlund C, Kristensson K, and Dallner G (1990) Lipid compositions of different regions of the human brain during aging. J. Neurochem 54, 415–23. [PubMed: 2299344]

(44). Funfschilling U, Saher G, Xiao L, Mobius W, and Nave KA (2007) Survival of adult neurons lacking cholesterol synthesis in vivo. BMC Neurosci. 8, 1. [PubMed: 17199885]

(45). Correa-Cerro LS, and Porter FD (2005) 3beta-hydroxysterol Delta7-reductase and the Smith-Lemli-Opitz syndrome. Mol. Genet. Metab 84, 112–26. [PubMed: 15670717]

(46). Xu L, Mirnics K, Bowman AB, Liu W, Da J, Porter NA, and Korade Z (2012) DHCEO accumulation is a critical mediator of pathophysiology in a Smith-Lemli-Opitz syndrome model. Neurobiol. Dis 45, 923–9. [PubMed: 22182693]

(47). Goudriaan A, Camargo N, Carney KE, Oliet SH, Smit AB, and Verheijen MH (2014) Novel cell separation method for molecular analysis of neuron-astrocyte co-cultures. Front. Cell. Neurosci 8, 12. [PubMed: 24523672]

(48). Rapp A, Gmeiner B, and Huttinger M (2006) Implication of apoE isoforms in cholesterol metabolism by primary rat hippocampal neurons and astrocytes. Biochimie 88, 473–83. [PubMed: 16376010]

(49). Acimovic J, Lovgren-Sandblom A, Monostory K, Rozman D, Golicnik M, Lutjohann D, and Bjorkhem I (2009) Combined gas chromatographic/mass spectrometric analysis of cholesterol precursors and plant sterols in cultured cells. J. Chromatogr. B: Anal. Technol. Biomed. Life Sci 877, 2081–6.

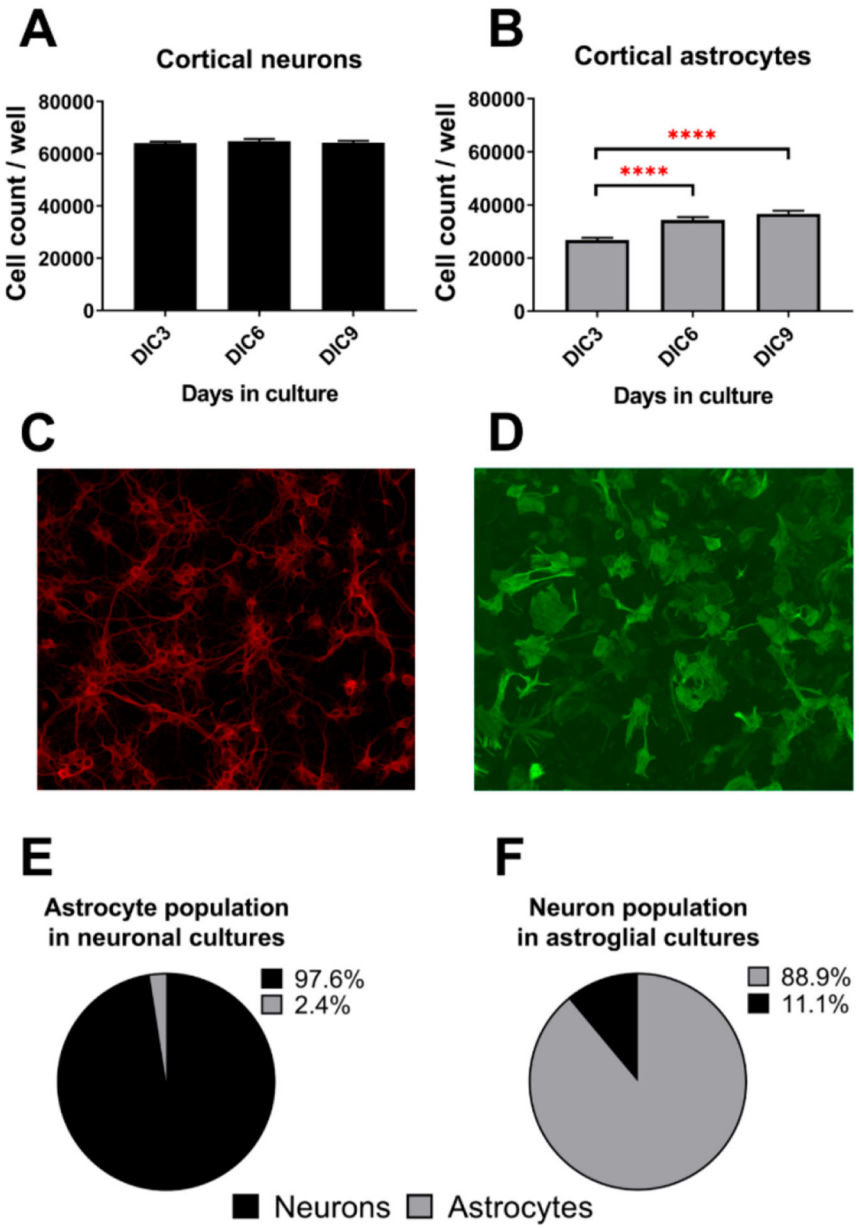

Figure 1.

Neuronal and astroglial cultures. Panels A and B show cell counts of neurons and astrocytes at different time points, respectively. Panels C and D show representative images of neurons and astrocytes in the culture wells. Neurons were labeled with anti-MAP2 antibody while astrocytes were stained with anti-GFAP antibody. Images were acquired with 20× and 40× objectives, respectively. Panels E and F denote the percent of astrocytes in neuronal cultures and the percent of neurons in astroglial cultures at 6 days in culture (DIC6), respectively. The absolute numbers of neurons and astrocytes in cultures, with statistical measures, are reported in Supplemental Table 1.

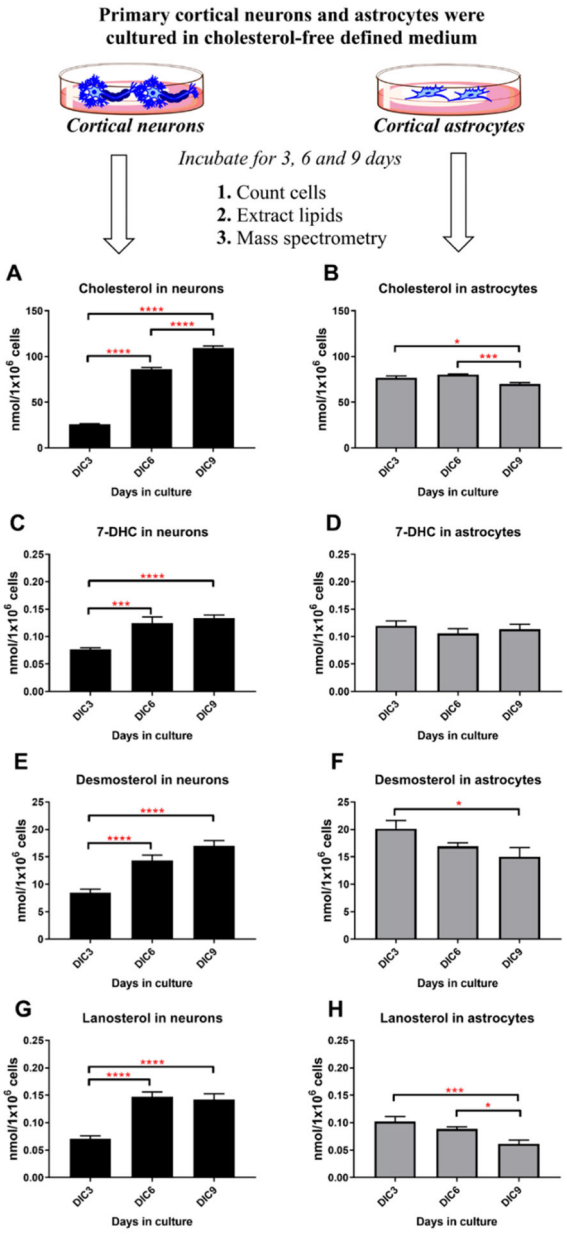

Figure 2.

Cortical neurons endogenously synthesize cholesterol. Primary neurons and astrocytes were incubated for 3, 6, and 9 days in defined cholesterol-free medium. Levels of cholesterol, 7-DHC, desmosterol and lanosterol levels were measured by LC-MS/MS. Panels on the left show neuronal sterols (A, C, E, G), while panels on the right denote astrocytic sterol levels (B, D, F, H). Sterol levels were normalized to the total cell count at the end point of each experiment. Sterol values correspond to the mean ± SEM of 8–12 replicates. Statistical significance is denoted by asterisks (*$p < 0.05$; ***$p < 0.001$; ****$p < 0.0001$). Note that all sterols accumulate in neurons in a time-dependent manner and that a similar process is not observed in astrocytes.

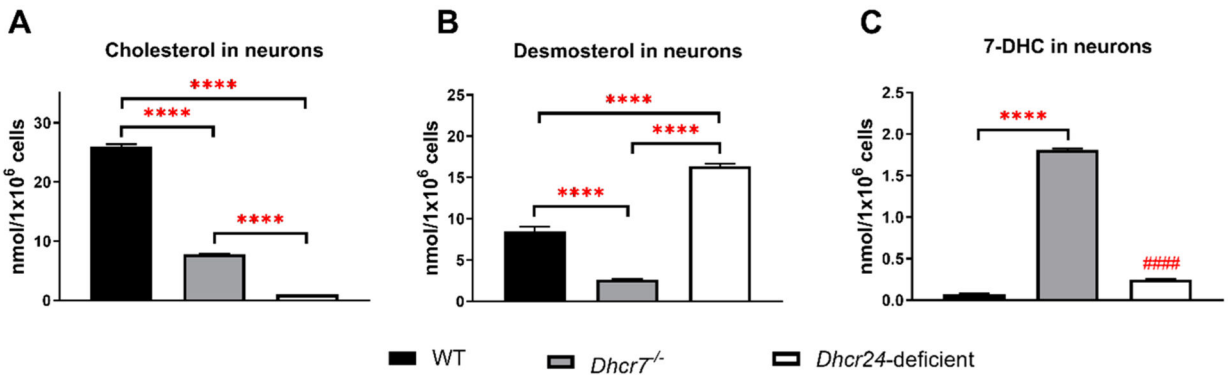

Figure 3.

Accumulation of sterol intermediates in *Dhcr7*$^{-/-}$and *Dhcr24*-deficient neurons. Comparison of cholesterol (A), desmosterol (B), and 7-DHC (C) levels between WT, *Dhcr7*$^{-/-}$, and *Dhcr24*-deficient neurons (*Dhcr24*$^{-/-}$). Neurons were cultured in defined cholesterol-free medium for 3 days and subjected to LC-MS/MS. Values correspond to mean ± SEM of 8–12 replicates. In all panels, statistical significance between individual groups is denoted by asterisks (****$p < 0.0001$); #### denotes the difference between WT and *Dhcr24*-deficient neurons ($p < 0.0001$).

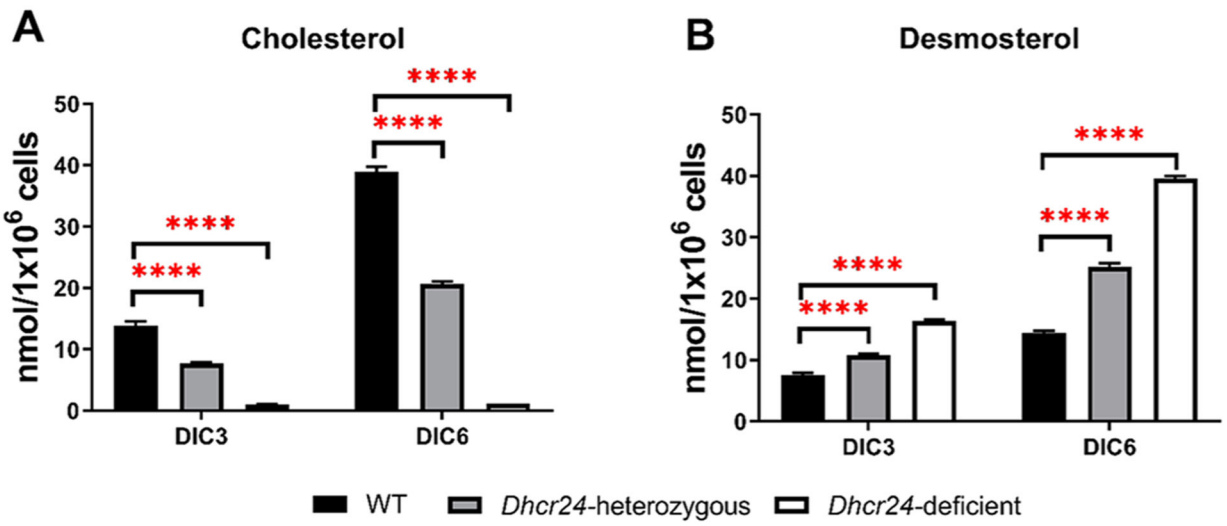

Figure 4.

Desmosterol replaces cholesterol in *Dhcr24*$^{-/-}$neurons in a time-dependent manner. WT (*Dhcr*$^{+/+}$), *Dhcr24*-heterozygous (*Dhcr24*$^{\pm}$), and *Dhcr24*-deficient (*Dhcr24*$^{-/-}$) neurons were cultured in defined cholesterol-free medium and cholesterol (A) and desmosterol (B) levels were assayed at DIC3 and DIC6. Values correspond to mean ± SEM of 8–12 replicates. In all panels, statistical significance between individual groups is denoted by asterisks (****$p <$ 0.0001). Note that in *Dhcr24*$^{-/-}$ neurons, cholesterol is fully replaced by desmosterol.

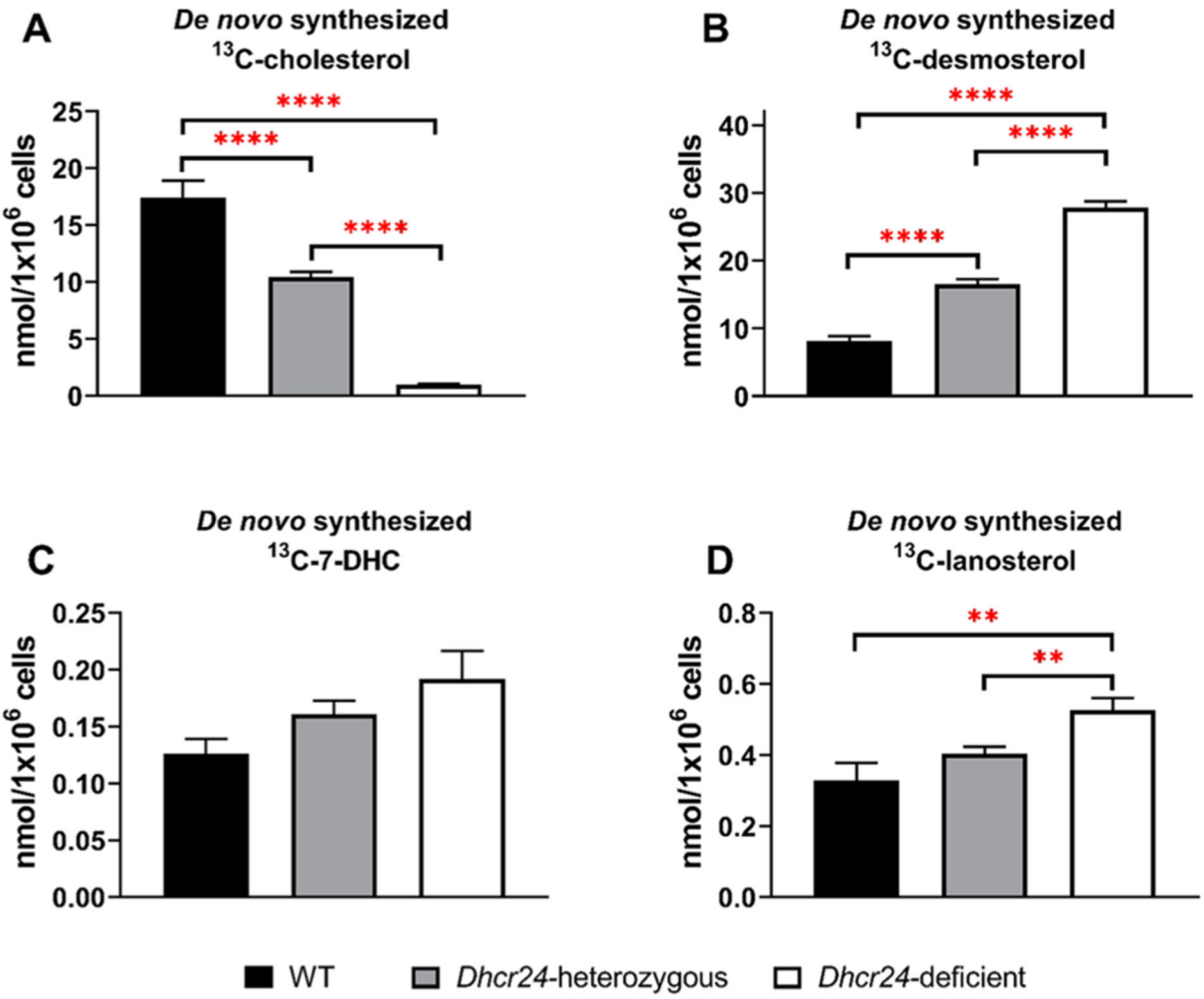

Figure 5.

Assessing active de novo cholesterol synthesis in neurons using $^{13}C_6$-glucose. Profile of selected de novo synthesized sterols in WT and *Dhcr24* mutant neurons (*Dhcr24*$^{\pm}$ and *Dhcr24*$^{-/-}$). Neurons were cultured in defined cholesterol-free medium where glucose was replaced by $^{13}C_6$-glucose. ^{13}C-labeled sterols were analyzed at DIC6. Values of ^{13}C-labeled cholesterol (A), desmosterol (B), 7-DHC (C), and lanosterol (D) correspond to mean ± SEM of 8–12 replicates. In all panels, statistical significance is denoted by asterisks (**$p < 0.01$; ****$p < 0.0001$).

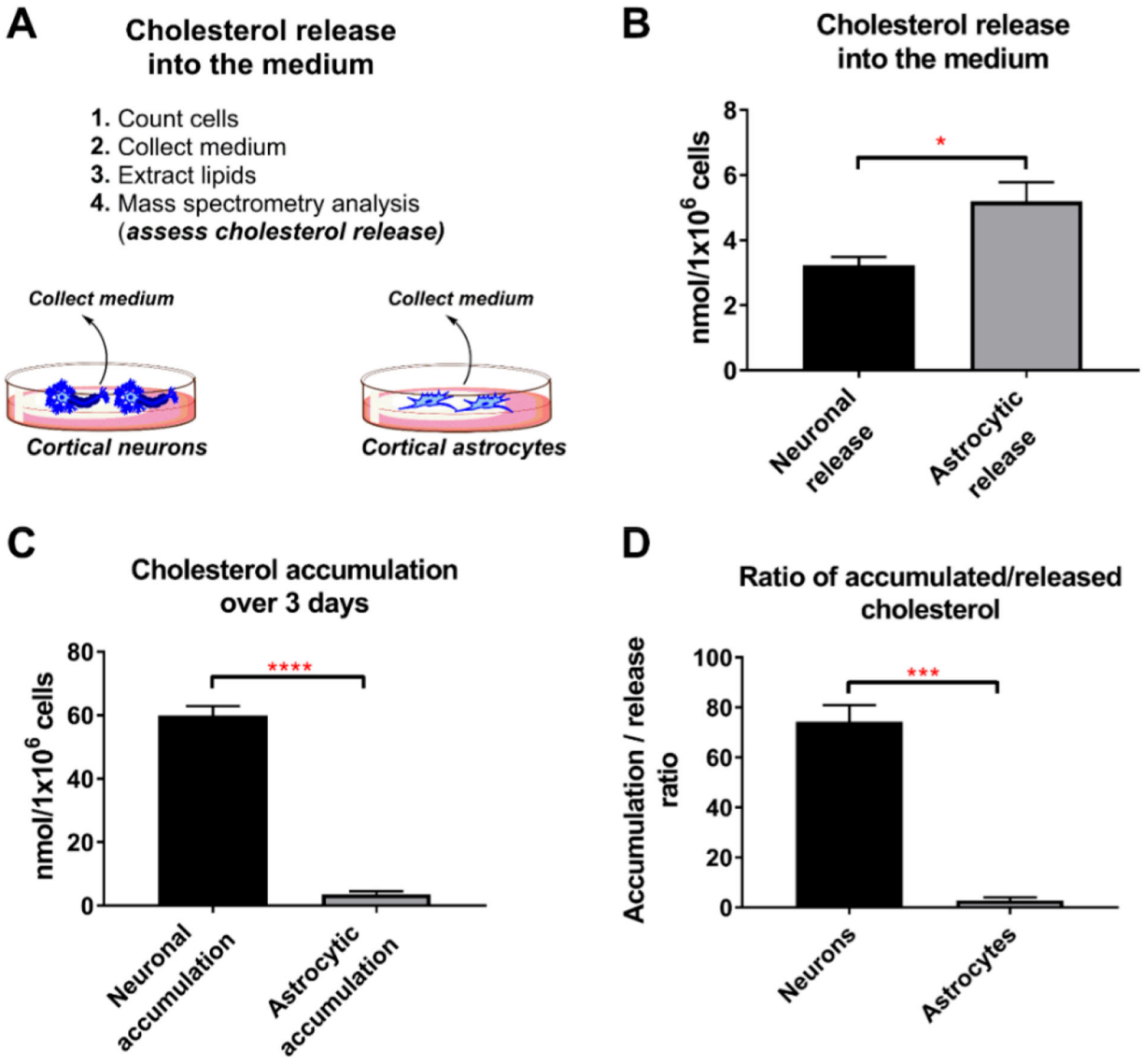

Figure 6.

Astrocytes release more cholesterol than neurons. (A) Total cholesterol detected in the medium over 3 days in culture. Both neuronal and astroglial cells were cultured in a defined cholesterol-free medium. (B) Analyzed media were collected at DIC6 and reflect the release of cholesterol between DIC3 and DIC6. Cholesterol levels were normalized to the total cell count at DIC6. Values correspond to the mean ± SEM of 3 replicates. Note that astrocytes release 60% more cholesterol than neurons. (C) Increase in total cholesterol in neurons and astrocytes over a 3 day period. Values correspond to the mean ± SEM of 8 replicates. Note that neurons accumulated 17-fold more cholesterol than astrocytes over the 3 day period. (D) Ratio of accumulated over released cholesterol over a 3 day period. Note that neurons retain the vast majority of their newly synthesized cholesterol, while astroglial cells release more cholesterol than they accumulate. Values correspond to the mean ± SEM of 8 replicates. In all panels, statistical significance is denoted by asterisks (*$p < 0.05$, ***$p < 0.001$; ****$p < 0.0001$).

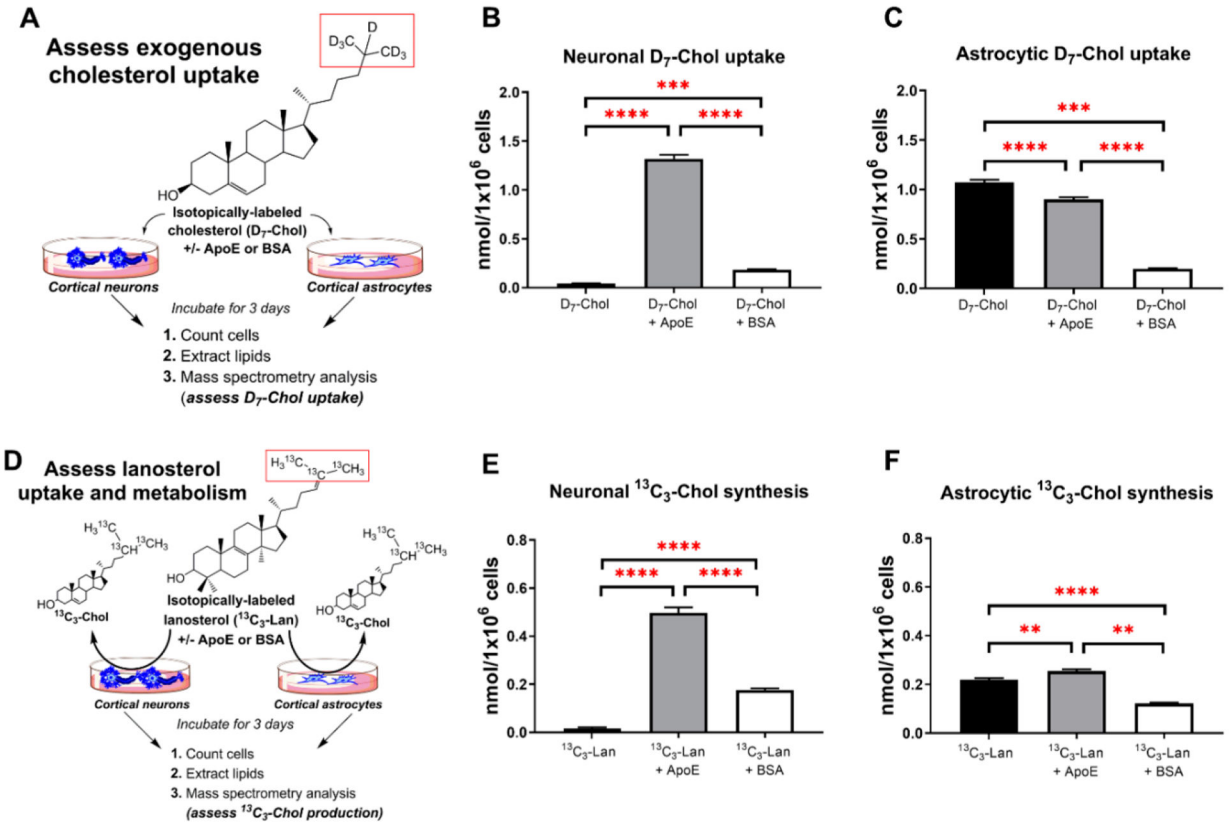

Figure 7.

Neuronal and astrocytic uptake of exogenous sterols. Neurons and astrocytes were cultured in defined cholesterol-free medium supplemented with free isotopically labeled cholesterol (D_7-Chol), D_7-Chol precomplexed with ApoE, and D_7-Chol precomplexed with BSA as illustrated in Panel A. The labeled moiety is highlighted in red. Final concentration of D_7-Chol in all conditions was 500 nM; protein final concentration was 0.7 μg/mL (either ApoE or BSA). Panels B and C show the uptake of D_7-Chol from the medium by neurons and astrocytes, respectively. D_7-Chol levels were normalized to the total cell count at the end point of the experiment (DIC3). Sterol values correspond to the mean ± SEM of 8–12 replicates. Note that ApoE facilitates the uptake of D_7-Chol by neurons but not by astrocytes. Panel D denotes the experimental design to test the incorporation of $^{13}C_3$−Lanosterol by neurons and astrocytes. Cells were cultured in defined cholesterol-free medium and with free isotopically labeled lanosterol ($^{13}C_3$−Lan), $^{13}C_3$−Lan precomplexed with ApoE, and $^{13}C_3$−Lan precomplexed with BSA. The labeled moiety is highlighted in red. Panels E and F show $^{13}C_3$−Chol levels derived from the conversion of $^{13}C_3$−Lan by neurons and astrocytes, respectively. $^{13}C_3$−Chol levels were normalized to the total cell count at the end point of each experiment. Sterol values correspond to the mean ± SEM of 8–12 replicates. Note that the uptake and conversion of lanosterol into cholesterol is 40-fold higher in neurons when lanosterol is precomplexed with ApoE, while in astrocytes the same treatment increases only by 15%. In all panels, statistical significance is denoted by asterisks (**$p < 0.01$, ***$p < 0.001$; ****$p < 0.0001$).

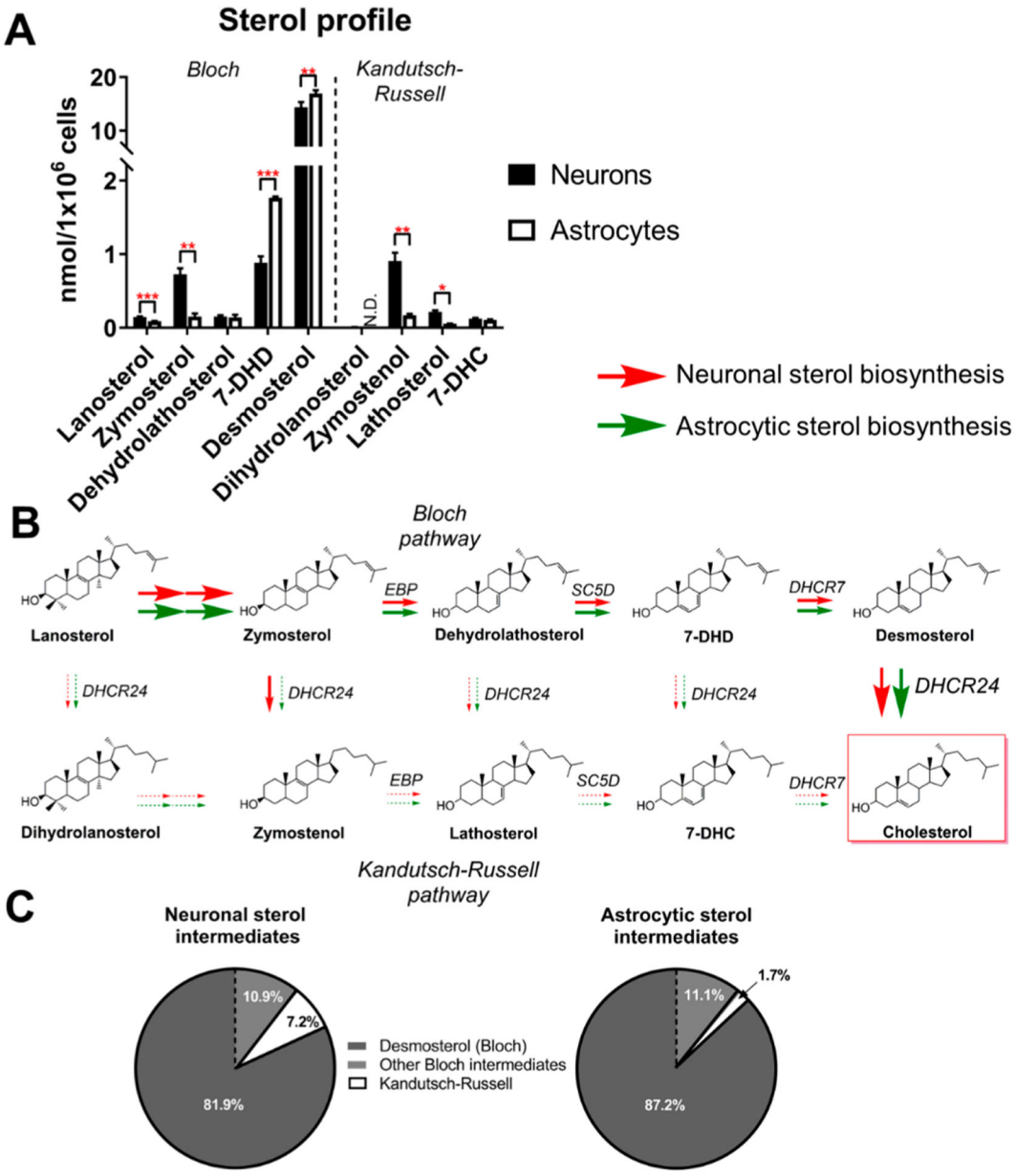

Figure 8.

Both neurons and astrocytes synthesize cholesterol via the Bloch pathway. (A) GC-MS profile of postlanosterol cholesterol biosynthesis intermediates in cultured neurons and astrocytes. Cells were cultured in a defined cholesterol-free medium. Intermediates in the Bloch pathway are shown on the left, while those from the Kandutsch-Russell pathway are depicted on the right of the graph. Sterol levels were determined at DIC6 and values correspond to mean ± SEM of 3 replicates. Statistical significance is denoted by asterisks (*$p < 0.05$, **$p < 0.01$, ***$p < 0.001$, ND − nondetectable). (B) Schematic representation depicting the preferential routes for the conversion of lanosterol into cholesterol by cultured neurons and astrocytes. Red and green arrows represent the pathways utilized by neurons and astrocytes, respectively. Arrow thickness corresponds to the strength of pathway

utilization. (C) Pie chart representation denoting the percent of Bloch and Kandutsch-Russell intermediates in cultured neurons and astrocytes at DIC6. Note that desmosterol is the most abundant intermediate in both neurons and astrocytes and that both cell types have higher levels of intermediates from the Bloch pathway, suggesting that the Kandutsch-Russell pathway utilization is miniscule at this developmental stage.